Inclusion of Interference Terms in the Amati-Bertocchi-Fubini-Stanghellini-Tonin Multiperipheral Model*

DALE R. SNIDER† AND DON M. TOW
Lawrence Radiation Laboratory, University of California, Berkeley, California 94720
(Received 11 September 1970)

An important class of interference terms is included in the ABFST multiperipheral model by adding an extra term to the inhomogeneous term and to the kernel of the integral equation. This additional term corresponds to the contribution to the 2-to-4 cross section from interchanging one or two pairs of particles from two different vertices. It is found that these interference terms change only slightly the position of the output vacuum pole, although they give a non-negligible contribution to the four-particle production cross section.

I. INTRODUCTION

ONE of the popular approximations of multiperipheral models is to neglect interference terms arising from the overlap of amplitudes with different particle orderings along the multiperipheral chain. Supporting, but not proving, this assumption is the fact that the multiperipheral amplitude is largest when the longitudinal momenta are ordered according to the particles' position along the chain.

Recent calculations[1–3] with the ABFST multiperipheral model,[4] the only multiperipheral model without arbitrary normalization of the kernel, have found the kernel to be too weak by a factor of 2 to 5 to explain the intercepts of Regge trajectories. These calculations neglected all interference except that inherent in a 2-to-2 process.

Because of the basic assumption of the multiperipheral model, we expect interference terms to be inversely ordered in importance according to their complexity. In this paper we study the effect of including in the model the "next order" interference. This is incorporated in the model by adding the interference terms from the 2-to-4 cross section to the kernel of the integral equation.

We find that including this interference has only a small effect on the position of the output vacuum pole; this, however, does not mean that for high-multiplicity production cross sections interference effects are negligible.

Since interference terms in the ABFST multiperipheral model have their origin in Bose statistics of the final-state pions, we begin in Sec. II by studying the effects of symmetry on production amplitudes (ignoring isospin until Sec. III); we then derive the modified integral equation and a formula to measure the effect on the position of output Regge poles when a certain class of interference terms is included. Isospin is then properly taken into account in Sec. III. Section IV discusses the 2-to-2 π-π amplitudes that we use as input. We discuss the results in Sec. V. In the Appendix, we discuss four-particle phase space and the kinematic variables used in our calculation.

II. MODIFIED INTEGRAL EQUATION FOR ABSORPTIVE PART

In this section we consider pions to be isospinless. The basic assumption of the ABFST multiperipheral model is that the amplitude for two pions to go to n pions (n must be even because of G parity) is given by

$$T_n(p_1,p_2,\ldots,p_n;\,p_a,p_b) = [(q_1^2-\mu^2)(q_2^2-\mu^2)\cdots(q_{(n/2)-1}^2-\mu^2)]^{-1} \times T_2(p_1,p_2;\,p_a,q_1)T_2(p_3,p_4;\,-q_1,q_2)\cdots \times T_2(p_{n-1},\,p_n;\,-q_{(n/2)-1},\,p_b), \quad (2.1)$$

where

$$q_i=\sum_{j=1}^{2i} p_j-p_a,$$

μ is the pion mass, and $T_2(p_k,p_l;\,q_i,q_j)$ is the off-shell 2-to-2 π-π scattering amplitude. A diagram illustrating the variables and representing Eq. (2.1) is shown in Fig. 1.

If we neglect all interference terms due to different orderings of the final-state particles, then the amplitude in (2.1) may be successfully squared and integrated to get the 2-to-n cross section. However, since pions obey Bose statistics, (2.1) is not a proper amplitude. A

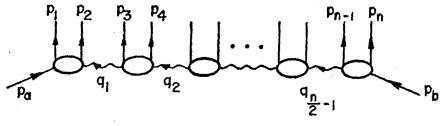

FIG. 1. Schematic representation of Eq. (2.1) for the 2-to-n amplitude, showing factorization and momentum assignment. Each blob is an off-shell 2-to-2 amplitude.

* Work supported in part by the U. S. Atomic Energy Commission.
† Present address: Physics Department, University of Wisconsin-Milwaukee, Milwaukee, Wis.
[1] D. M. Tow, Phys. Rev. D 2, 154 (1970).
[2] G. F. Chew, T. Rogers, and D. R. Snider, Phys. Rev. D 2, 765 (1970).
[3] G. F. Chew and D. R. Snider, Phys. Rev. D 1, 3453 (1970).
[4] L. Bertocchi, S. Fubini, and M., Tonin, Nuovo Cimento 25, 626 (1962); D. Amati, A. Stanghellini, and S. Fubini, *ibid.* 26, 896 (1962).

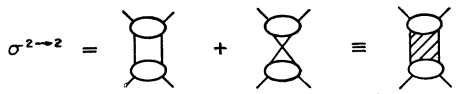

FIG. 2. 2-to-2 cross section.

properly symmetrized amplitude is

$$M_n(p_1,p_2,\ldots,p_n;\,p_a,p_b)=\sum_{i=1}^{n!} T_n(\mathcal{P}_i(\{p_j\});\,p_a,p_b), \quad (2.2)$$

where $\mathcal{P}_i(\{p_j\})$ is the ith permutation of the set of n momenta $(p_1,p_2,\ldots,p_n)$. The 2-to-n cross section is

$$\sigma^{2\to n}(s)=\frac{1}{2\lambda(s,m_a^2,m_b^2)(2\pi)^{3n-4}}\frac{1}{n!}\int d\Phi_n \times\Big[\sum_{i=1}^{n!} T_n(\mathcal{P}_i(\{p_j\});\,p_a,p_b)\Big]^* \times\Big[\sum_{k=1}^{n!} T_n(\mathcal{P}_k(\{p_j\});\,p_a,p_b)\Big], \quad (2.3)$$

where s is the c.m. energy squared and Φ_n is the n-particle phase space and is given by

$$\Phi_n=\prod_{i=1}^{n}\left[\int d^4p_i\,\delta^+(p_i^2-m_i^2)\right]\delta^4\Big(p_a+p_b-\sum_{i=1}^{n} p_i\Big). \quad (2.4)$$

The factor $1/n!$ in (2.3) comes from normalizing the final-state vector or, equivalently, from integrating only once over the distinguishable region of phase space. Since the p_j's are variables of integration, (2.3) may be rewritten in the unsymmetric form

$$\sigma^{2\to n}(s)=\frac{1}{2\lambda(s,m_a^2,m_b^2)(2\pi)^{3n-4}}\int d\Phi_n \times T_n^*(p_1,p_2,\ldots,p_n;\,p_a,p_b) \times\Big[\sum_{k=1}^{n!} T_n(\mathcal{P}_k(\{p_j\});\,p_a,p_b)\Big]. \quad (2.5)$$

The usual assumption of the ABFST model is that only those $2^{n/2}$ permutations corresponding to interchanging pions from the same vertex are kept in (2.5).[5]

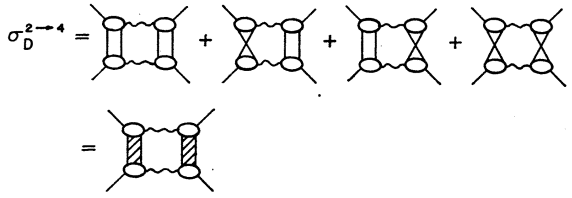

FIG. 3. The terms in $\sigma^{2\to4}$ from the permutations of D. We call this sum the uncrossed diagram.

[5] Throughout the rest of this paper, we call this the "standard assumption."

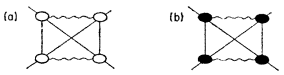

FIG. 4. (a) One of the terms from the class C; the other 15 terms are represented by interchanging two intermediate lines from one of the four vertices. (b) Sum of all 16 terms of C. We call this the single-crossed diagram.

With this assumption, the 2-to-n cross section becomes

$$\sigma^{2\to n}(s)=\frac{1}{2\lambda(s,m_a^2,m_b^2)(2\pi)^{3n-4}}\int d\Phi_n \times T_2^*(p_1,p_2;\,p_a,q_1)[T_2(p_1,p_2;\,p_a,q_1)+T_2(p_2,p_1;\,p_a,q_1)] \times(q_1^2-\mu^2)^{-2}T_2^*(p_3,\,p_4;\,-q_1,\,q_2) \times[T_2(p_3,\,p_4;\,-q_1,\,q_2)+T_2(p_4,\,p_3;\,-q_1,\,q_2)] \times(q_2^2-\mu^2)^{-2}\times\cdots\times[q_{(n/2)-1}^2-\mu^2]^{-2} \times T_2^*(p_{n-1},\,p_n;\,-q_{(n/2)-1},p_b) \times[T_2(p_{n-1},\,p_n;\,-q_{(n/2)-1},\,p_b) +T_2(p_n,\,p_{n-1};\,-q_{(n/2)-1},\,p_b)]. \quad (2.6)$$

This leads to the usual integral equation[4] for the forward absorptive part of the elastic amplitude with the kernel being proportional to the 2-to-2 cross section. This 2-to-2 cross section is schematically represented in Fig. 2. For $n=2$, (2.5) is identical to (2.6). But for $n=4$, (2.5) has additional terms not contained in (2.6). It is these additional interference terms to the 2-to-4 cross section with which we are primarily concerned. For each production cross section a general class of interference terms will be included in the model when we add these 2-to-4 interference terms to the previous kernel.

For $n=4$, there are 24 permutations in (2.5). This set of 24 permutations may be separated into three convenient classes by defining the set of permutation operators $D=\{I,S_{12},S_{34},S_{12}S_{34}\}$, where I is the identity operator and S_{ij} is the operator which interchanges the i and j indices. Then $\{\mathcal{P}_k\}=D+C+X$, where $C\equiv DS_{23}D$ and $X\equiv DS_{13}S_{24}$. The sets D, C, and X contain four, 16, and four permutations, respectively. Notice that applying any of the operators in D does not change the expression for $q_1\equiv p_1+p_2-p_a\equiv p_b-p_3-p_4$; this is why this particular decomposition of $\{\mathcal{P}_k\}$ is useful here.

The terms in $\sigma^{2\to4}$ from the permutations of D are exactly those included in the ABFST model under the

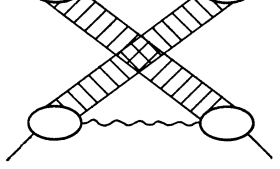

FIG. 5. Sum of all four terms in X. We call this the double-crossed diagram.

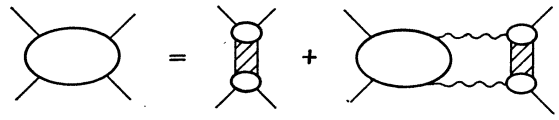

FIG. 6. Schematic representation of the integral equation for the forward absorptive part of the elastic amplitude under the "standard assumption."

"standard assumption." These four terms are shown in Fig. 3. One of the 16 terms in C is shown in Fig. 4(a); the other 15 terms are obtained by interchanging two final-state particles from one of the four vertices. We represent the sum of all these 16 terms of C by Fig. 4(b). The sum of all four terms from the class X is represented by Fig. 5. These interference terms from classes C and X are the terms not included under the standard assumption.

If we define

$$q_D\equiv p_1+p_2-p_a,\ q_C\equiv p_1+p_3-p_a,\ q_X\equiv p_3+p_4-p_a, \quad (2.7)$$

and use the abbreviated notation $T_{12,aD}\equiv T_2(p_1,p_2;p_a,q_D)$, etc., then we may write

$$\sigma^{2\to4}=\sigma_D{}^{2\to4}+\sigma_C{}^{2\to4}+\sigma_X{}^{2\to4},$$

where

$$\sigma_D{}^{2\to4}(s)=\frac{1}{2\lambda(s,m_a{}^2,m_b{}^2)(2\pi)^8}\int d\Phi_4\frac{1}{(q_D{}^2-\mu^2)^2}\times T_{12,aD}{}^*(T_{12,aD}+T_{21,aD})\times T_{34,-Db}{}^*(T_{34,-Db}+T_{43,-Db}), \quad (2.8a)$$

$$\sigma_C{}^{2\to4}(s)=\frac{1}{2\lambda(s,m_a{}^2,m_b{}^2)(2\pi)^8}\int d\Phi_4\frac{1}{(q_D{}^2-\mu^2)(q_C{}^2-\mu^2)}\times(T_{12,aD}{}^*+T_{21,aD}{}^*)\times(T_{34,-Db}{}^*+T_{43,-Db}{}^*)(T_{13,aC}+T_{31,aC})\times(T_{24,-Cb}+T_{42,-Cb}), \quad (2.8b)$$

$$\sigma_X{}^{2\to4}(s)=\frac{1}{2\lambda(s,m_a{}^2,m_b{}^2)(2\pi)^8}\int d\Phi_4\frac{1}{(q_D{}^2-\mu^2)(q_X{}^2-\mu^2)}\times T_{12,aD}{}^*(T_{12,-Xb}+T_{21,-Xb})\times T_{34,-Db}{}^*(T_{34,aX}+T_{43,aX}). \quad (2.8c)$$

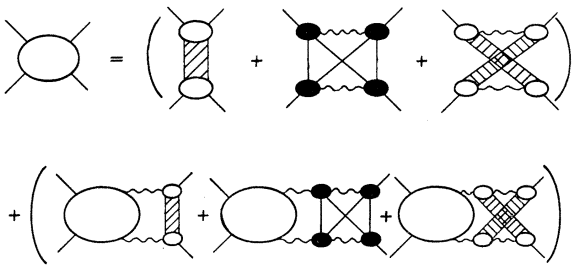

FIG. 7. Schematic representation of modified integral equation when interference terms from classes C and X are included.

From these equations, we easily see that the antisymmetric part of the 2-to-2 amplitude gives zero contribution. Therefore, we can express (2.8) in terms of the symmetric 2-to-2 amplitudes, M_2, defined by Eq. (2.2). At this point it is also convenient to switch from momentum variables to kinematics invariants. Since each 2-to-2 amplitude has one particle off shell, it is a function of three invariants. As in the Appendix, we define

$$s_{ij}\equiv(p_i+p_j)^2,\quad t_{ia}\equiv(p_i-p_a)^2,\quad t_{ib}\equiv(p_b-p_i)^2,\quad \tau_\nu\equiv q^2{}_\nu,\ \text{for}\ \nu=D,C,X. \quad (2.9)$$

We may rewrite (2.8) as

$$\sigma_D{}^{2\to4}(s)=\frac{1}{2\lambda(s,m_a{}^2,m_b{}^2)(2\pi)^8}\int d\Phi_4\times\frac{|M_2(s_{12},t_{1a},\tau_D)|^2|M_2(s_{34},t_{4b},\tau_D)|^2}{4(\tau_D-\mu^2)^2}, \quad (2.10a)$$

$$\sigma_C{}^{2\to4}(s)=\frac{1}{2\lambda(s,m_a{}^2,m_b{}^2)(2\pi)^8}\int d\Phi_4\frac{1}{(\tau_D-\mu^2)(\tau_C-\mu^2)}\times M_2{}^*(s_{12},t_{1a},\tau_D)M_2{}^*(s_{34},t_{4b},\tau_D)\times M_2(s_{13},t_{1a},\tau_C)M_2(s_{24},t_{4b},\tau_C), \quad (2.10b)$$

$$\sigma_X{}^{2\to4}(s)=\frac{1}{2\lambda(s,m_a{}^2,m_b{}^2)(2\pi)^8}\int d\Phi_4\frac{1}{4(\tau_D-\mu^2)(\tau_X-\mu^2)}\times M_2{}^*(s_{12},t_{1a},\tau_D)M_2{}^*(s_{34},t_{4b},\tau_D)\times M_2(s_{12},t_{2b},\tau_X)M_2(s_{34},t_{3a},\tau_X). \quad (2.10c)$$

In the Appendix, eight invariants are chosen as independent, and expressions for all the others are derived in terms of these eight. The four-particle phase space is also expressed in terms of these independent variables.

Having found the corrections to the 2-to-4 cross section, we proceed to investigate the correction to the

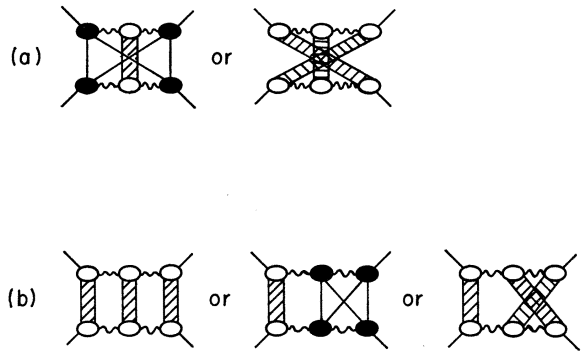

FIG. 8. (a) Diagrams not generated by the kernel of this paper. (b) Diagrams generated by the kernel, which give a larger contribution than the diagrams in (a).

total cross section due to including these effects in the integral equation. The integral equation for the forward absorptive part of the elastic amplitude under the standard assumption is schematically represented in Fig. 6. We modify this integral equation by adding the interference terms C and X to the kernel and to the inhomogeneous term. This modified integral equation is schematically represented in Fig. 7. At this point it should be mentioned that this new kernel cannot generate diagrams of the form shown in Fig. 8(a). However, because these diagrams involve interchanging lines from non-neighboring vertices, they are expected to give a smaller contribution than the diagrams of Fig. 8(b), which can be generated by this kernel. Our kernel also cannot generate diagrams of the form shown in Fig. 9(a). This diagram may give a comparable contribution to the diagram of Fig. 9(b), since both diagrams involve crossing four lines into their neighboring vertices. Diagrams of the form of Fig. 9(a) can be included by adding further terms to the kernel. If we want to include all interference terms, then the kernel is actually an infinite series. It is hoped that the magnitude of this first modification gives an indication of the rate of convergence of this series.

To study the effect on the position of the output poles from changing the kernel of the integral equation we examine the diagonalized integral equation, which can be written as[2]

$$F^J(\tau,\tau')=F_0{}^J(\tau,\tau')+\int_{-\infty}^{0}d\tau''F^J(\tau,\tau'')K^J(\tau'',\tau'), \tag{2.11}$$

where

$$K^J(\tau,\tau')=\frac{1}{16\pi^3}\times\frac{1}{(\tau-\mu^2)^2}\int_{4\mu^2}^{\infty}ds \times\frac{\lambda(s,\mu^2,\mu^2)e^{-(J+1)\eta(s,\tau,\tau')}\sigma(s)}{J+1}, \tag{2.12}$$

with

$$\cosh\eta(s,\tau,\tau')=(s-\tau-\tau')/2(\tau\tau')^{1/2},$$
$$\lambda(a,b,c)=(a^2+b^2+c^2-2ab-2ac-2bc)^{1/2},$$

and $\sigma(s)$ is the π-π cross section to be included in the kernel. For our case, we have (see Fig. 7)

$$\sigma(s)=\sigma^{2\to2}(s)+\sigma_C{}^{2\to4}(s)+\sigma_X{}^{2\to4}(s). \tag{2.13}$$

Because we are concerned with the relative effect of including a correction, we will avoid all intricacies of solving the integral equation. For the Fredholm determinant $D(J)$, whose vanishing determines the pole position, we use the trace approximation, i.e.,

$$D(J)\approx1-\int d\tau\, K^J(\tau,\tau). \tag{2.14}$$

By making certain approximations, Chew, Rogers, and

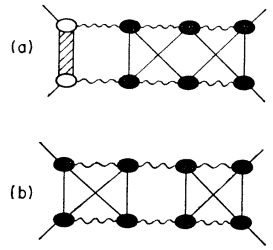

FIG. 9. (a) Diagram not generated by the kernel of this paper. (b) Diagram generated by the kernel, which may give a contribution comparable to that in (a).

Snider[2] found a particularly simple expression for the trace for J near 1. It gives

$$D(J)=1-2R/J(J+1)(J+2), \tag{2.15}$$

where

$$R=\frac{1}{16\pi^3}\int_{4\mu^2}^{s_{\max}}ds\,\sigma(s). \tag{2.16}$$

The approximations are (a) the trace approximation, (b) neglecting the high-energy tail of $\sigma^{el}(s)$ [in our calculation we set $\sigma^{el}(s)=0$ for $s>3$ GeV^2], and (c) neglecting the pion mass in doing the τ integration. Besides these approximations, there was also the choice of off-shell prescription. As in Ref. 2, we let the off-shell continuation be completely contained in θ, the c.m. scattering angle, i.e.,

$$M_2(s,\theta)_{\text{off-shell}}=M_2(s,\theta(s,t,\tau,\tau')). \tag{2.17}$$

This prescription leads to a simple relation between the two-particle contribution to the kernel and the π-π elastic cross section. Other equally plausible prescriptions lead to less-manageable relations. For the four-

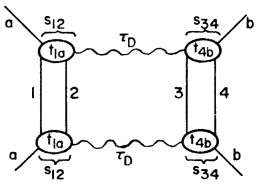

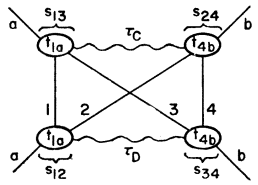

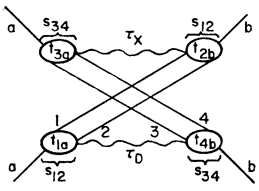

FIG. 10. Various kinematic invariants.

particle contribution to the kernel, we calculated its magnitude when the external lines are on shell.[6]

Finally, from Eqs. (2.16) and (2.13) we see that a measure of the effect on the position of the output pole by including interference terms is

$$\frac{\Delta R}{R^{\mathrm{el}}} \equiv \int ds[\sigma_C{}^{2\to 4}(s)+\sigma_X{}^{2\to 4}(s)] \Big/ \int ds\, \sigma^{2\to 2}(s). \quad (2.18)$$

III. INCLUDING ISOSPIN

We now consider the problem of isospin alone. Later we will see how to take into account both isospin and statistics. The kinematic invariants for all three diagrams are shown in Fig. 10. We work out the procedure in some detail for the uncrossed diagram; the procedure is the same for the crossed diagrams. The isospin indices for the uncrossed diagram are shown in Fig. 11.

Following the notation of Chew and Mandelstam,[7] and defining T_i to be the 2-to-2 amplitude at the ith vertex, and for each i defining A_i, B_i, and C_i to be three independent amplitudes at the ith vertex, we have

$$\begin{aligned}
T_{\mathrm{I}}(s_{12},t_{1a},\tau_D) &= A_{\mathrm{I}}\delta_{af}\delta_{ek}+B_{\mathrm{I}}\delta_{ae}\delta_{fk}+C_{\mathrm{I}}\delta_{ak}\delta_{ef},\\
T_{\mathrm{II}}(s_{34},t_{4b},\tau_D) &= A_{\mathrm{II}}\delta_{bf}\delta_{gj}+B_{\mathrm{II}}\delta_{bg}\delta_{fj}+C_{\mathrm{II}}\delta_{bj}\delta_{fg},\\
T_{\mathrm{III}}(s_{34},t_{4b},\tau_D) &= A_{\mathrm{III}}\delta_{ch}\delta_{gj}+B_{\mathrm{III}}\delta_{cg}\delta_{hj}+C_{\mathrm{III}}\delta_{cj}\delta_{gh},\\
T_{\mathrm{IV}}(s_{12},t_{1a},\tau_D) &= A_{\mathrm{IV}}\delta_{dh}\delta_{ek}+B_{\mathrm{IV}}\delta_{de}\delta_{hk}+C_{\mathrm{IV}}\delta_{dk}\delta_{eh},
\end{aligned} \quad (3.1)$$

where A_i's, B_i's, and C_i's have the same arguments as T_i's. The individual vertex amplitude of a definite isospin in the t channel is given by

$$\begin{aligned}
(T_i)_0 &= 3B_i+A_i+C_i,\\
(T_i)_1 &= A_i-C_i,\\
(T_i)_2 &= A_i+C_i,
\end{aligned} \quad (3.2)$$

where the subscript outside the parenthesis refers to the t-channel isospin at the ith vertex.

The 2-to-4 amplitude squared is given by

$$|T|^2=\sum[T_{\mathrm{I}}{}^*T_{\mathrm{II}}{}^*T_{\mathrm{III}}T_{\mathrm{IV}}/(\tau_D-\mu^2)^2],$$

where the sum is over all nonexternal isospin indices. The expression $|T|^2$ has 81 terms and can be written as

$$|T|^2=[1/(\tau_D-\mu^2)^2](A\delta_{ab}\delta_{cd}+B\delta_{ad}\delta_{bc}+C\delta_{ac}\delta_{bd}), \quad (3.3)$$

where A has 30 terms, B has 20 terms, and C has 31 terms. As we are mainly interested in the change in the position of the output vacuum pole, we consider only the case in which the isospin in the t channel is zero. This gives

$$|T|^2_{I_t=0}=[1/(\tau_D-\mu^2)^2](3B+A+C). \quad (3.4)$$

From isospin conservation we also know that

$$\begin{aligned}
|T|^2_{I_t=0}=[1/(\tau_D-\mu^2)^2][&a(T_{\mathrm{I}})_0{}^*(T_{\mathrm{II}})_0{}^*(T_{\mathrm{III}})_0(T_{\mathrm{IV}})_0\\
&+b(T_{\mathrm{I}})_0{}^*(T_{\mathrm{II}})_2{}^*(T_{\mathrm{III}})_2(T_{\mathrm{IV}})_0\\
&+b(T_{\mathrm{I}})_2{}^*(T_{\mathrm{II}})_0{}^*(T_{\mathrm{III}})_0(T_{\mathrm{IV}})_2\\
&+c(T_{\mathrm{I}})_1{}^*(T_{\mathrm{II}})_0{}^*(T_{\mathrm{III}})_0(T_{\mathrm{IV}})_1\\
&+c(T_{\mathrm{I}})_0{}^*(T_{\mathrm{II}})_1{}^*(T_{\mathrm{III}})_1(T_{\mathrm{IV}})_0\\
&+d(T_{\mathrm{I}})_1{}^*(T_{\mathrm{II}})_1{}^*(T_{\mathrm{III}})_1(T_{\mathrm{IV}})_1\\
&+e(T_{\mathrm{I}})_2{}^*(T_{\mathrm{II}})_1{}^*(T_{\mathrm{III}})_1(T_{\mathrm{IV}})_2\\
&+e(T_{\mathrm{I}})_1{}^*(T_{\mathrm{II}})_2{}^*(T_{\mathrm{III}})_2(T_{\mathrm{IV}})_1\\
&+f(T_{\mathrm{I}})_2{}^*(T_{\mathrm{II}})_2{}^*(T_{\mathrm{III}})_2(T_{\mathrm{IV}})_2].
\end{aligned} \quad (3.5)$$

Since (3.4) and (3.5) must be true for all A_i's, B_i's, and C_i's, we can equate the two expressions and thereby determine the unknown coefficients in (3.5). We find[8]

$$a=\tfrac{1}{9},\quad b=5/9,\quad c=\tfrac{1}{3},\quad d=1,\quad e=5/3,\quad f=25/9. \quad (3.6)$$

Similarly, we can derive analogous equations for the two crossed diagrams. The single-crossed diagram is given by

$$\begin{aligned}
|T|^2_{I_t=0}=&[1/(\tau_D-\mu^2)(\tau_C-\mu^2)]\\
&\times[\tfrac{1}{9}(T_{\mathrm{I}})_0{}^*(T_{\mathrm{II}})_0{}^*(T_{\mathrm{III}})_0(T_{\mathrm{IV}})_0\\
&+(5/9)(T_{\mathrm{I}})_0{}^*(T_{\mathrm{II}})_2{}^*(T_{\mathrm{III}})_2(T_{\mathrm{IV}})_0\\
&+(5/9)(T_{\mathrm{I}})_2{}^*(T_{\mathrm{II}})_0{}^*(T_{\mathrm{III}})_0(T_{\mathrm{IV}})_2\\
&-\tfrac{1}{3}(T_{\mathrm{I}})_1{}^*(T_{\mathrm{II}})_0{}^*(T_{\mathrm{III}})_0(T_{\mathrm{IV}})_1\\
&-\tfrac{1}{3}(T_{\mathrm{I}})_0{}^*(T_{\mathrm{II}})_1{}^*(T_{\mathrm{III}})_1(T_{\mathrm{IV}})_0\\
&+\tfrac{1}{2}(T_{\mathrm{I}})_1{}^*(T_{\mathrm{II}})_1{}^*(T_{\mathrm{III}})_1(T_{\mathrm{IV}})_1\\
&+(5/6)(T_{\mathrm{I}})_2{}^*(T_{\mathrm{II}})_1{}^*(T_{\mathrm{III}})_1(T_{\mathrm{IV}})_2\\
&+(5/6)(T_{\mathrm{I}})_1{}^*(T_{\mathrm{II}})_2{}^*(T_{\mathrm{III}})_2(T_{\mathrm{IV}})_1\\
&+(5/18)(T_{\mathrm{I}})_2{}^*(T_{\mathrm{II}})_2{}^*(T_{\mathrm{III}})_2(T_{\mathrm{IV}})_2],
\end{aligned} \quad (3.7)$$

where

$$\begin{aligned}
T_{\mathrm{I}} &= T_{\mathrm{I}}(s_{12},t_{1a},\tau_D),\\
T_{\mathrm{II}} &= T_{\mathrm{II}}(s_{34},t_{4b},\tau_D),\\
T_{\mathrm{III}} &= T_{\mathrm{III}}(s_{24},t_{4b},\tau_C),\\
T_{\mathrm{IV}} &= T_{\mathrm{IV}}(s_{13},t_{1a},\tau_C).
\end{aligned} \quad (3.8)$$

The double-crossed diagram is given by

$$\begin{aligned}
|T|^2_{I_t=0}=&[1/(\tau_D-\mu^2)(\tau_X-\mu^2)]\\
&\times\tfrac{1}{9}(T_{\mathrm{I}})^0{}^*(T_{\mathrm{II}})^0{}^*(T_{\mathrm{III}})^0(T_{\mathrm{IV}})^0\\
&+\tfrac{1}{3}(T_{\mathrm{I}})^0{}^*(T_{\mathrm{II}})^1{}^*(T_{\mathrm{III}})^0(T_{\mathrm{IV}})^1\\
&+\tfrac{1}{3}(T_{\mathrm{I}})^1{}^*(T_{\mathrm{II}})^0{}^*(T_{\mathrm{III}})^1(T_{\mathrm{IV}})^0\\
&+\tfrac{1}{2}(T_{\mathrm{I}})^1{}^*(T_{\mathrm{II}})^1{}^*(T_{\mathrm{III}})^1(T_{\mathrm{IV}})^1\\
&+(5/9)(T_{\mathrm{I}})^0{}^*(T_{\mathrm{II}})^2{}^*(T_{\mathrm{III}})^0(T_{\mathrm{IV}})^2\\
&+(5/9)(T_{\mathrm{I}})^2{}^*(T_{\mathrm{II}})^0{}^*(T_{\mathrm{III}})^2(T_{\mathrm{IV}})^0\\
&-(5/6)(T_{\mathrm{I}})^1{}^*(T_{\mathrm{II}})^2{}^*(T_{\mathrm{III}})^1(T_{\mathrm{IV}})^2\\
&-(5/6)(T_{\mathrm{I}})^2{}^*(T_{\mathrm{II}})^1{}^*(T_{\mathrm{III}})^2(T_{\mathrm{IV}})^1\\
&+(5/18)(T_{\mathrm{I}})^2{}^*(T_{\mathrm{II}})^2{}^*(T_{\mathrm{III}})^2(T_{\mathrm{IV}})^2],
\end{aligned} \quad (3.9)$$

[6] This is an approximation, since using Eq. (2.17) for the 2-to-2 amplitude to calculate the 2-to-4 cross section does not lead to a 2-to-4 cross section that is independent of the mass of the external pions.

[7] G. F. Chew and S. Mandelstam, Phys. Rev. 119, 467 (1960).

[8] Equation (3.5) is also true with the same coefficients as those of Eq. (3.6) if the isospin indices are taken as s-channel isospins. The freedom of interchanging s- and t-channel isospin indices occurs only for the uncrossed diagram.

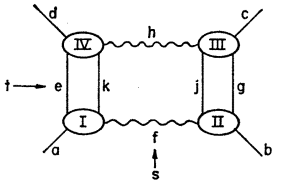

FIG. 11. Isospin indices for the uncrossed diagram.

where the superscript outside the parenthesis refers to the s-channel isospin at the ith vertex and

$$\begin{aligned} T_{\mathrm{I}} &= T_{\mathrm{I}}(s_{12},t_{1a},\tau_D), \\ T_{\mathrm{II}} &= T_{\mathrm{II}}(s_{34},t_{4b},\tau_D), \\ T_{\mathrm{III}} &= T_{\mathrm{III}}(s_{12},t_{2b},\tau_X), \\ T_{\mathrm{IV}} &= T_{\mathrm{IV}}(s_{34},t_{3a},\tau_X). \end{aligned} \tag{3.10}$$

Combining the results of this section and Sec. II, we see that to include both isospin and statistics just means that we should replace the numerators of Eqs. (2.10a)–(2.10c) by the terms in the brackets in Eqs. (3.5), (3.7), and (3.9), respectively. Of course, the t-channel isospin will now appear as an index in Eqs. (2.11)–(2.16) and (2.18).

IV. π-π AMPLITUDES

From Eq. (2.10) and the discussion in Sec. III, we see that we need as input the 2-to-2 π-π amplitude for all three isospins with one of the pions off shell. As was discussed in Refs. 1–3, the low-energy contribution must be the dominant contribution in generating the output poles. Therefore, in this paper we input only S waves (both $I=0$ and $I=2$), P wave, and D wave ($I=0$ only), and leave out the Pomeranchuk tail by setting the amplitudes equal to zero for $s>3$ GeV^2.

For the P wave and D wave, we use Breit-Wigner terms with widths equal to 140 MeV and with $m_\rho=765$ MeV and $m_f=1260$ MeV as their resonance masses, respectively. Since these two partial-wave amplitudes must behave near threshold as k^{2l+1}, where k is the magnitude of the c.m. momentum, we multiply the Breit-Wigner terms by

$$\left(\frac{k^2(s)}{s}\right)^{(2l+1)/2}\left(\frac{4s_R}{s_R-4\mu^2}\right)^{(2l+1)/2}, \tag{4.1}$$

where $s_R=m_\rho{}^2$ and $l=1$ for the P wave, and $s_R=m_f{}^2$ and $l=2$ for the D wave. The factor (4.1) is chosen such that it is normalized to unity at the resonance mass and has constant asymptotic behavior.

For the S waves we use the phase shifts shown in Figs. 12 and 13.[9] Because of the uncertainty in the $I=0$ S-wave phase shift, we have used two different forms. The form $(\delta_0{}^0)_{\mathrm{I}}$ corresponds to a broad resonance at the mass of the ρ. The $(\delta_0{}^0)_{\mathrm{II}}$ does not correspond to a resonance, but rather it asymptotically approaches 90°.

[9] We thank Robert D. Mathews for suggestions on the phase shifts.

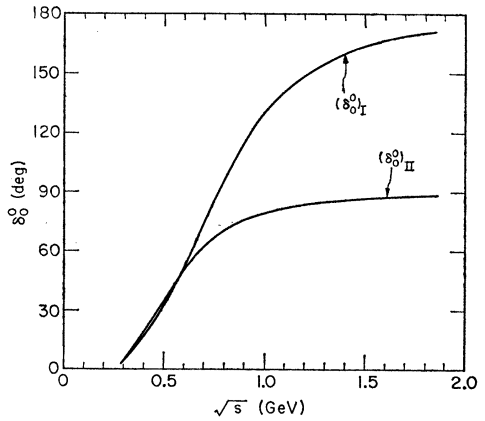

FIG. 12. $(\delta_0{}^0)_{\mathrm{I}}$ and $(\delta_0{}^0)_{\mathrm{II}}$ as a function of $s^{1/2}$.

All these S-wave amplitudes have scattering lengths near the current-algebra values.[10] Since there is some indication[11,12] that the S-wave off-shell scattering lengths may be larger than the on-shell values, we also tried S-wave partial-wave amplitudes with scattering lengths increased by a factor of 3. We find that although for small s the 2-to-4 cross sections become larger, all essential features of our results remain unchanged.

V. RESULTS

Using Monte Carlo integration, we calculated the 2-to-4 cross sections for $I_t=0$ from the classes D, C, and X. The results for classes C and X are shown in Figs. 14(a) and 14(b), respectively. As is expected, class C in general gives a smaller contribution than class X, since the former splits up the resonances. The result for class D and the sum of the results for classes C and X are shown in Fig. 15. We see that for low energy, the contribution of the interference terms is not negligible. But as the energy increases, the crossed terms drop off faster with s than the uncrossed term, because at high s the momenta of the final particles can be very different, and so interchanging two such momenta can greatly increase the momentum transfers. We also find that the two different forms of $\delta_0{}^0$ do not give rise to different results until s gets large, when $(\delta_0{}^0)_{\mathrm{I}}$ gives a small amplitude, whereas $(\delta_0{}^0)_{\mathrm{II}}$ gives a large amplitude.

To calculate the effect on the position of the output vacuum pole, we calculated $\Delta R_0/R_0{}^{\mathrm{el}}$ defined in Eq.

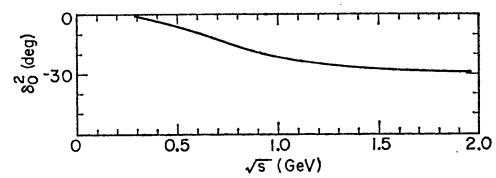

FIG. 13. $\delta_0{}^2$ as a function of $s^{1/2}$.

[10] S. Weinberg, Phys. Rev. Letters **17**, 616 (1966).
[11] G. Wolf, Phys. Rev. **182**, 1538 (1969).
[12] F. Wagner, Nuovo Cimento **64A**, 189 (1969).

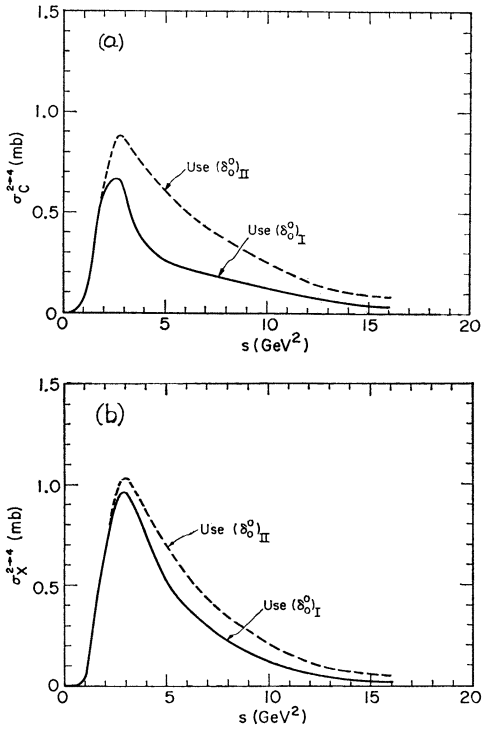

FIG. 14. $\sigma_C^{2\to4}(s)$ and $\sigma_X^{2\to4}(s)$ for $I_t=0$. Solid curve uses $(\delta_0^0)_I$ as input, and dashed curve uses $(\delta_0^0)_{II}$. (a) $\sigma_C^{2\to4}(s)$. (b) $\sigma_X^{2\to4}(s)$.

(2.18), where the subscript specifies the t-channel isospin. We find

$$\frac{\Delta R_0}{R_0^{el}} \approx \begin{cases} 0.06, \text{ if } (\delta_0^0)_I \text{ is used} \\ 0.08, \text{ if } (\delta_0^0)_{II} \text{ is used.} \end{cases} \tag{5.1}$$

Using the numerical calculations of Ref. 1, we find[13] that corresponding to this 6–8% increase in the kernel strength, the output vacuum pole changes only from

$$\alpha_{I=0}=0.30 \quad \text{to} \quad \alpha_{I=0}=0.33. \tag{5.2}$$

The smallness of this correction to the kernel indicates

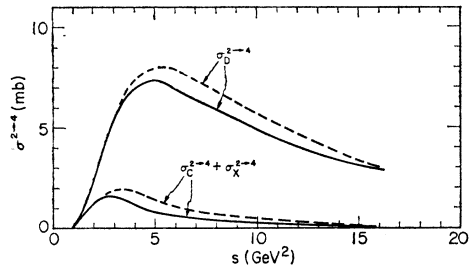

FIG. 15. $\sigma_D^{2\to4}(s)$ and $\sigma_C^{2\to4}(s)+\sigma_X^{2\to4}(s)$ for $I_t=0$. Solid curves use $(\delta_0^0)_I$ as input, and dashed curves use $(\delta_0^0)_{II}$.

[13] We could have used Eq. (2.15) to calculate the position of the output pole. However, because of the approximations used in deriving (2.15), this method of calculating output pole position is not so accurate as the numerical calculation of Ref. 1.

that the infinite series of the kernel (as discussed in Sec. II) most probably converges rapidly.

Our relative magnitude of the interference terms to the noninterference term in the 2-to-4 cross section is probably consistent with the recent result of Jurewicz *et al.*,[14] who found that the contribution to the cross section from the set of all interference terms for the reaction $\pi^+p \to p\,3\pi^+\,2\pi^-$ at 8 GeV/c is about 80% of the contribution from the noninterference term. We expect their effect to be much larger than ours because there are more interference terms for $n=6$ than for $n=4$, and because they include all interference terms, whereas we include only a subset (although the important subset).

That interference terms are important in calculating n-particle production cross sections but not important in calculating the position of the output vacuum pole is understandable because

$$\sigma^{\text{total}}(s)=\sum_n \sigma^n(s) \propto s^{(\alpha_{I=0}-1)}, \tag{5.3}$$

which shows that a small change in $\alpha_{I=0}$ can give rise to a large change in $\sigma^n(s)$ for large s.

In conclusion, although the inclusion of interference terms can greatly increase n-particle production cross sections for large n, it does not alter appreciably the positions of the output Regge poles. Therefore, another mechanism must be sought to strengthen the kernel of the ABFST multiperipheral integral equation. One possible mechanism is the inclusion of K-meson exchange.

ACKNOWLEDGMENTS

We thank G. F. Chew and S.-S. Shei for discussions.

APPENDIX: PHASE SPACE AND KINEMATIC VARIABLES

Although n-body phase space has previously been worked out by others, for completeness we include a discussion of four-body phase space in this appendix [most of the material in this Appendix was worked out by one of the authors (D. R. S.) in collaboration with Terence Rogers]. We define n-body phase space as

$$\Phi_n=\prod_{i=1}^{n}\left[\int d^4p_i\,\delta^+(p_i^2-m_i^2)\right]\delta^4(p_a+p_b-\sum_{i=1}^{n} p_i). \tag{A1}$$

Two-body phase space may be written as

$$\Phi_2(s;m_a^2,m_b^2;m_1^2,m_2^2)=\frac{\lambda(s,m_1^2,m_2^2)}{8s}\int d\Omega$$

$$=\frac{1}{4\lambda(s,m_a^2,m_b^2)}\int dt d\phi, \tag{A2}$$

[14] A. Jurewicz, L. Michejda, J. Namyslewski, and J. Turnau, Warsaw report, 1970 (unpublished).

where

$$s=(p_a+p_b)^2,\quad \lambda(a,b,c)=(a^2+b^2+c^2-2ab-2ac-2bc)^{1/2},$$
$$d\Omega=d\cos\theta d\phi,$$

and θ and ϕ are the scattering angles in the c.m. system.

We want to consider four-particle phase space as a nested set of two-particle phase spaces. The kinematic variables are shown in Fig. 16. For this purpose we define

$$P_i=\sum_{j=1}^{i} p_j,\quad v_i=P_i^2$$

and (A3)

$$q_i=P_i-p_a,\quad t_i=q_i^2.$$

We will now show that the four-body phase space can be written as

$$\Phi_2(p_a+p_b\to p_4+P_3)\Phi_2(p_a+q_3\to p_3+P_2)\times\Phi_2(p_a+q_2\to p_1+p_2),$$

with extra integrals over v_2 and v_3. We start at the p_4 end and lump the other three final-state particles together by using

$$\delta^4(p_1+p_2+p_3+p_4-p_a-p_b)=\int d^4P_3\,\delta^4(P_3+p_4-p_a-p_b)\delta^4(p_1+p_2+p_3-P_3)$$

and also

$$\int d^4P_3=\int dv_3\int d^4P_3\,\delta^+(P_3^2-v_3).$$

Inserting these into Eq. (A1) for Φ_4, we obtain

$$\Phi_4=\int dv_3\Big[\int d^4P_3\,\delta^+(P_3^2-v_3)\int d^4p_4\,\delta^+(p_4^2-m_4^2)\times\delta^4(P_3+p_4-p_a-p_b)\Big]\Big[\int d^4p_1\,\delta^+(p_1^2-m_1^2)\times\int d^4p_2\,\delta^+(p_2^2-m_2^2)\int d^4p_3\,\delta^+(p_3^2-m_3^2)\times\delta^4(p_1+p_2+p_3-q_3-p_a)\Big]$$
$$=\int dv_3\,\Phi_2(P_a+p_b\to P_3+p_4)\times\Phi_3(p_a+q_3\to p_1+p_2+p_3).$$

Now for fixed P_3 (and hence q_3) we repeat this step for Φ_3. That is, we use

$$\delta^4(p_1+p_2+p_3-p_a-q_3)=\int dv_2\int d^4P_2\,\delta^+(P_2^2-v_2)\times\delta^4(P_2+p_3-p_a-q_3)\delta^4(p_1+p_2-P_2)$$

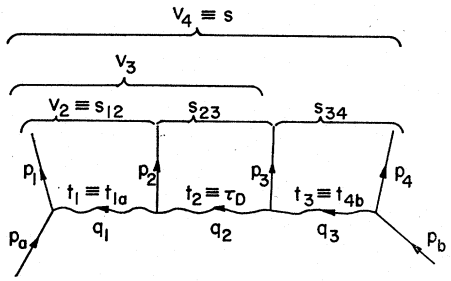

FIG. 16. Description of assignment of momenta and kinematic invariants.

to get

$$\Phi_3(p_a+q_3\to p_1+p_2+p_3)=\int dv_2\,\Phi_2(p_a+q_3\to P_2+p_3)\Phi_2(p_a+q_2\to p_1+p_2).$$

This gives for Φ_4 (when the Φ's are expressed in terms of invariants)

$$\Phi_4(s;m_a^2,m_b^2;m_1^2,m_2^2,m_3^2,m_4^2)=\int dv_2\int dv_3\,\Phi_2(s;m_a^2,m_b^2;v_3,m_4^2)\times\Phi_2(v_3;m_a^2,t_3;v_2,m_3^2)\Phi_2(v_2;m_a^2,t_2;m_1^2,m_2^2).$$

We evaluate each Φ_2 in the c.m. frame of the system it describes to get

$$\Phi_4=\int dv_3\frac{\lambda(s,v_3,m_4^2)}{8s}\int d\Omega_3\int dv_2\frac{\lambda(v_3,v_2,m_3^2)}{8v_3}\times\int d\Omega_2\frac{\lambda(v_2,m_1^2,m_2^2)}{8v_2}\int d\Omega_1. \quad \text{(A4)}$$

Here θ_i is the angle between P_i and p_a in the c.m. frame of q_{i+1} and p_a, and ϕ_i is the azimuthal angle between P_i and p_{i+2} in the same system; ϕ_3 is an irrelevant angle. For each $d\Omega$ the range of integration is 4π, and for the v's the range is where all the λ's are positive.

We could have used the other form of two-body phase space, Eq. (A2), to get

$$\Phi_4=\int\frac{dv_3dt_3d\phi_3}{4\lambda(s,m_a^2,m_b^2)}\int\frac{dv_2dt_2d\phi_2}{4\lambda(v_3,t_3,m_a^2)}\times\int\frac{dt_1d\phi_1}{4\lambda(v_2,t_2,m_a^2)}, \quad \text{(A5)}$$

but now the range over the t's is more complicated. To calculate the range in t_i for fixed v_{i+1}, v_i, and t_{i+1}, we

use the equation

$$\cos\theta_i=\frac{v_{i+1}(v_{i+1}+2t_i-m_a^2-t_{i+1}-v_i-m_{i+1}^2)+(m_a^2-t_{i+1})(v_i-m_{i+1}^2)}{\lambda(v_{i+1},m_a^2,t_{i+1})\lambda(v_{i+1},v_i,m_{i+1}^2)}, \tag{A6}$$

and set $\cos\theta_i=1$ and -1.

We need to be able to express any kinematic variables in terms of those chosen here. In particular we want to find expressions for the various Mandelstam invariants in terms of the set of v's, t's, and ϕ's. The first step in this is to express the two-particle "subenergies" s_{23} and s_{34} of Fig. 16 in terms of this set.

Consider the diagram in Fig. 17. Now, ϕ_{i-1} is the azimuthal angle for the two-body reaction $q_i+p_a\to p_i+P_{i-1}$. That is, it is the azimuthal angle between $\mathbf{P}_{i-1}$ and $\mathbf{p}_{i+1}$ in the frame where $\mathbf{P}_i=\mathbf{p}_a+\mathbf{q}_i=0$ and where $\mathbf{p}_a$ is along the $+z$ direction, as shown in Fig. 18. From an examination of this we see that the two-particle subenergy $s_{i,i+1}\equiv(p_i+p_{i+1})^2$ is a function of ϕ_i. To find this function we write

$$\begin{aligned}s_{i,i+1}\equiv(p_i+p_{i+1})^2&=(P_{i+1}-P_{i-1})^2\\&=v_{i+1}+v_{i-1}-2P_{i+1}{}^0P_{i-1}{}^0+2|\mathbf{P}_{i+1}||\mathbf{P}_{i-1}|\\&\quad\times(\cos\psi\cos\theta_{i-1}+\sin\psi\sin\theta_{i-1}\cos_{i-1}),\end{aligned} \tag{A7}$$

where we have introduced the angle ψ shown in Fig. 18. To find ψ, we use

$$t_{i+1}=q_{i+1}{}^2=(q_i+p_{i+1})^2=t_i+m_{i+1}{}^2+2q_i{}^0p_{i+1}{}^0+2|\mathbf{q}_i||\mathbf{p}_{i+1}|\cos\psi. \tag{A8}$$

For these two equations we need a number of energies and three-vector magnitudes in this frame of reference. In general, if

$$k_1\pm k_2=k_3,\quad \mathbf{k}_3=0,\quad \text{and}\quad k_i{}^2=x_i\quad \text{for}\quad i=1,\,2,\,3,$$

then

$$|\mathbf{k}_1|=|\mathbf{k}_2|=\lambda(x_1,x_2,x_3)/2x_3{}^{1/2},\quad k_1{}^0=\frac{x_1+x_3-x_2}{2x_3{}^{1/2}},$$

and

$$k_2{}^0=\pm\left(\frac{x_2+x_3-x_1}{2x_3{}^{1/2}}\right).$$

In our case we have

$$P_{i-1}+p_i=P_i,\quad P_{i+1}-p_{i+1}=P_i,\quad p_a+q_i=P_i,\quad \mathbf{P}_i=0.$$

Since we know all the momentum squares, we have the needed energies and three-momenta to find $\cos\psi$, and therefore $s_{i,i+1}$, in terms of ϕ_{i-1}.[15] After some algebra, from Eq. (A7) we find

$$s_{i,i+1}=v_{i+1}+v_{i-1}+\frac{-\mathrm{Det}(A)+2[G(\theta_{i-1})G(\psi)]^{1/2}\cos\phi_{i-1}}{\lambda^2(v_i,m_a^2,t_i)}, \tag{A9}$$

where

$$G(\theta_{i-1})=G(v_i,t_{i-1},m_a^2,t_i,v_{i-1},m_i^2)$$

and

$$G(\psi)=G(v_i,t_{i+1},m_a^2,t_i,v_{i+1},m_{i+1}^2),$$

with G being the Kibble function, given by

$$\begin{aligned}G(s,t,a,b,c,d)=&st(-s-t+a+b+c+d)\\&-s(a-c)(b-d)-t(a-b)(c-d)\\&-(ad-bc)(a+d-b-c).\end{aligned}$$

The matrix A in Eq. (A9) is

$$A=\begin{bmatrix}2v_i & v_i+m_a^2-t_i & v_i+v_{i+1}-m_{i+1}^2\\ v_i+m_a^2-t_i & m_a^2 & v_{i+1}+m_a^2-t_{i+1}\\ v_i+v_{i-1}-m_i^2 & v_{i-1}+m_a^2-t_{i-1} & 0\end{bmatrix}.$$

Next we would like to express all other two-body invariants in terms of our basic set, now taken to be v_2, v_3, t_1, t_2, t_3, s_{23}, s_{34}, and of course s. Once we have found the three-particle invariant $s_{234}\equiv(p_2+p_3+p_4)^2$, which is like v_3 but on the opposite side, the remaining two-particle invariants come simply. To find s_{234} we compress p_3 and p_4 together. Figure 19 shows this and s_{234}

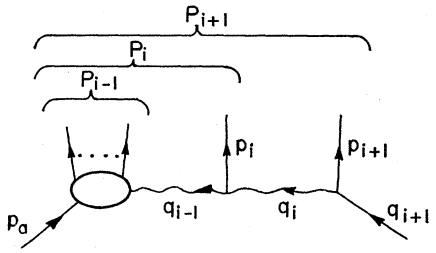

FIG. 17. General kinematics.

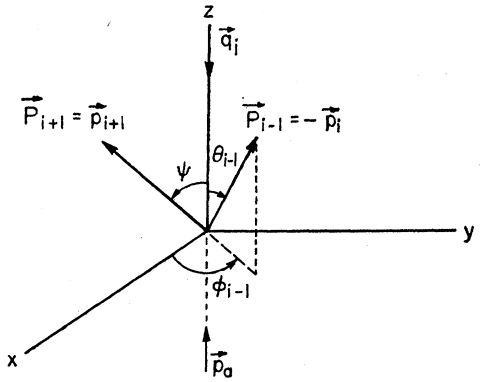

FIG. 18. Definition of variables in frame where $\mathbf{P}_i=0$.

[15] Another method for finding the expression for $\cos\psi$ is to use an analogy with a c.m. scattering angle θ. In general, to find $\cos\theta$ in terms of s, t, and the four masses, one uses $k_a+k_b=K=k_c+k_d$, $\mathbf{K}=0$, $s=K^2$, $t=k_a-k_c$, and θ is the angle between $\mathbf{k}_a$ and $\mathbf{k}_c$. From Figs. 17 and 18 we have $p_a+q_i=P_i=P_{i+1}+(-p_{i+1})$, $\mathbf{P}_i=0$, $v_i=P_i{}^2$, $t_{i+1}=(p_a-P_{i+1})^2$, and ψ is the angle between $\mathbf{p}_a$ and $\mathbf{P}_{i+1}$. Therefore, if $\cos\theta=f(s,t,m_a^2,m_b^2,m_c^2,m_d^2)$, then $\cos\psi=f(v_i,t_{i+1},m_a^2,t_i,v_{i+1},m_{i+1}^2)$.

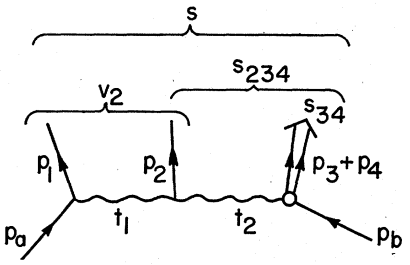

FIG. 19. Diagram for calculating s_{234}.

in relation to the known variables. From this figure we see that the calculation of s_{234} is completely analogous to the calculation of $s_{i,i+1}$. We immediately write the answer:

$$s_{234}=s+m_1^2+\frac{-\mathrm{Det}A'+2(G_1G_2)^{1/2}\cos\phi_1}{\lambda^2(v_2,m_a^2,t_2)}, \quad \text{(A10)}$$

where

$$G_1=G(v_2,t_1,m_a^2,t_2,m_1^2,m_2^2),$$
$$G_2=G(v_2,m_b^2,m_a^2,t_2,s,s_{34}),$$

and

$$A'=\begin{pmatrix} 2v_2 & v_2+m_a^2-t_2 & v_2+s-s_{34} \\ v_2+m_a^2-t_2 & m_a^2 & s+m_a^2-m_b^2 \\ v_2+m_1^2-m_2^2 & m_1^2+m_a^2-t_1 & 0 \end{pmatrix}.$$

The other two-body invariants can now be easily shown to be

$$s_{13}=v_3-v_2-s_{23}+m_1^2+m_2^2+m_3^2,$$
$$s_{24}=s_{234}-s_{23}-s_{34}+m_2^2+m_3^2+m_4^2,$$
$$t_{2b}=t_1-t_2-s_{234}+s_{34}+m_2^2+m_b^2,$$
$$t_{3a}=t_3-t_2-s_{123}+v_2+m_3^2+m_a^2,$$
$$\tau_C=m_2^2+m_3^2+t_1-t_2+t_3-s_{23},$$
$$\tau_X=m_a^2+m_b^2-t_2+v_2+s_{34}-s.$$

PHYSICAL REVIEW D VOLUME 3, NUMBER 4 15 FEBRUARY 1971

Crossed-Channel Partial-Wave Expansions and the Bethe-Salpeter Equation*

L. M. SAUNDERS AND O. H. N. SAXTON†
Joseph Henry Laboratories, Princeton University, Princeton, New Jersey 08540

AND

CHUNG-I TAN
Joseph Henry Laboratories, Princeton University, Princeton, New Jersey 08540
and
Physics Department,‡ Brown University, Providence, Rhode Island 02912

(Received 7 October 1970)

The Bethe-Salpeter equation for the direct-channel absorptive part of the scattering amplitude is analyzed in the ladder approximation to investigate the relationship between $SO(1,3)$ and $SO(1,2)$ crossed-channel partial-wave analyses. The $SO(1,2)$ expansion, used when the momentum transfer Q is spacelike, is studied in detail in the limit $Q_\mu \to 0$. The connection between the $SO(1,3)$ and $SO(1,2)$ partial-wave amplitudes at $Q_\mu=0$ is obtained explicitly, as is the familiar result that a Toller pole is equivalent to an infinite sequence of integrally spaced Regge poles at $Q_\mu=0$.

I. INTRODUCTION

PARTIAL-WAVE analyses of scattering amplitudes and dynamical equations in the crossed (t) channel offer a powerful formalism for studying directly the high-energy behavior of the scattering process in the direct (s) channel.[1] The functions of interest are expanded in matrix elements of representations of the little group of the momentum transfer vector Q, the underlying symmetry group of the reaction. An expansion coefficient, labeled by the values of the group's Casimir operators when restricted to a specific representation, is precisely what is meant by a partial-wave amplitude. If Q is spacelike ($Q^2<0$), as in nonforward scattering, the little group is $SO(1,2)$, and if Q is a null vector, as in the forward scattering of equal-mass particles, the little group is $SO(1,3)$. Because the representations, and therefore the expansions, are different, there is in general no obvious connection between the forward description and the nonforward description in the limit $Q_\mu \to 0$.

In this paper we discuss this connection in a simple model, the spinless Bethe-Salpeter equation for the absorptive part of the scattering amplitude, using a

* Research partially sponsored by the U. S. Air Force Office of Scientific Research under Contract No. AF 49(638)-1545 and partially by the U. S. Atomic Energy Commission under Contract No. NYO-2262TA-226.

† Present address: Stanford Linear Accelerator Center, Stanford University, Stanford, Calif. 94305.

‡ Present address.

[1] A good discussion and bibliography of past work is given in lectures by P. Winternitz at the Dublin Summer School (1969), Rutherford Laboratory Report No. RPP/T/3 (unpublished).